RESEARCH ARTICLE

Confined masonry as practical seismic construction alternative–the experience from the 2014 Cephalonia Earthquake

Fillitsa KARANTONI[a*], Stavroula PANTAZOPOULOU[b], Athanasios GANAS[c]

[a] Department of Civil Engineering, University of Patras, Rio Achaia 26504, Greece

[b] The Lassonde Faculty of Engineering, Deptartment of Civil Engineering, York University, Toronto M3J 1P3, Canada

[c] Institute of Geodynamics, National Observatory of Athens, Athens, Greece

*Corresponding author. E-mail: karmar@upatras.gr

ABSTRACT   During August 1953 three strong earthquakes of magnitude ranging from 6.3 to 7.2 shook the Ionian Island of Cephalonia (Kefalonia), Greece, and destroyed almost the entire building stock of the Island which consisted primarily of traditional unreinforced masonry (URM) houses. The authorities went on to restructuring of the building stock, using a structural system that is most like what is known today as confined masonry. They designed about 14 types of one- to two-storey buildings providing the engineers with detailed construction plans. These buildings are known as "Arogi" buildings (Arogi in Greek meaning Aid). On the 24th of January and 3rd of February 2014, two earthquakes of magnitude 6.1 and 6.0 struck the island, causing significant soil damages, developing excessively high ground accelerations. Surprisingly, no damage was reported in the "Arogi" buildings. The seismic behavior of the buildings is examined by FEM linear analysis and it is compared to that of URM structures. Computed results illustrate that the displacements of identical URM buildings would be about twice the magnitudes observed in the corresponding "Arogi" ones, with the implication that the earthquake sequence of 2014 would have caused critical damage should the type of structure be of the URM type. Furthermore, it is illustrated that this low cost alternative method of construction is a very effective means of producing earthquake resilient structures, whereas further reduction of seismic displacement may be achieved in the order of 50% with commensurate effects on damage potential, when reinforced slabs are used to replace the timber roofs.

KEYWORDS   Cephalonia, confined masonry, comparative FEM analysis, unreinforced masonry, seismic damage

1   Introduction

Cephalonia Island (Ionian Sea, Greece) is considered to be among the most active tectonic regions in Europe and one of the most active zones in the Eastern Mediterranean region. Cephalonia has been repeatedly subjected to strong ground shaking with near-fault characteristics, due to the proximity of the island to CTF (Cephalonia Transform Fault) [1–3]. The 100-km long NNE-SSW fault zone accommodates the relative motion of the Apulia (Africa) and Aegean (Eurasia) lithospheric plates, and has a GPS slip-rate estimated between 10 and 25 mm/yr [4]. Two recent, largest CTF events include the Jan. 17, 1983 ($M = $ 6.8; Ref. [1]) and the November 15, 2015 ($M = $ 6.5; Ref. [5]) strong ground motions.

On January 26, 2014, 13:55 GMT and on February 3, 2014, GMT 03:07 Cephalonia was struck by two strong, shallow earthquakes (National Observatory of Athens magnitudes Mw 6.1 and Mw 6.0, respectively). The second event generated the strongest ground motion that has ever been instrumentally recorded in Greece reaching ground accelerations in the range of 0.76 g [6]. The first earthquake was a deeper event (hypocenter at 16.5 km depth; [7]) whereas the second event was much more shallow (4.6 km according to seismological data, Karastathis et al. [7]; 3–5 km centroid depth from InSAR;

Boncori et al. [8]). The environmental effects triggered by the earthquakes were mainly concentrated in the western part of Cephalonia Island and particularly at the Palliki peninsula (Fig. 1) where co-seismic horizontal displacements of 10–20 cm were measured by InSAR [8]. It must be noted that most environmental effects, induced by the first event of Jan. 26, were reactivated one week later by the second (Feb. 3) one. In particular, severe earthquake-induced slope failures e.g., rock falls and landslides were widespread in the western coast and south/central parts of Palliki, and in the east coast of Argostoli Bay (Fig. 1) while liquefaction phenomena were reported in reclaimed lands at the waterfront areas of Lixouri and Argostoli and induced severe damages to port facilities e.g. quay walls and piers, mainly at the port of Lixouri [9,10].

Fig. 1   The Cephalonia Transform Fault (CTF) and the epicenters (yellow stars) of the main events of the seismic sequence of January – February 2014

Structural damages in buildings particularly in the Palliki peninsula where the highest ground accelerations had been recorded were rather limited despite the excessive ground motion accelerations. Significant damages were observed in a few characteristic examples of deficient Reinforced Concrete (R.C.) buildings due to known inadequacies in the structural system (pilotis system with substandard detailing of transverse reinforcement and significant torsional eccentricities, see Figs. 2(a), and (b)). In all other cases, wherever damages were reported, they were concentrated in the infills of the affected buildings. In the same region, there were several structures comprising unreinforced masonry that had survived the 1953 earthquake whereas

they sustained significant damages in the 2014 earthquake (see Figs. 2(c) and (d)). However, the number of significantly damaged structures was rather small considering the extent and volume of the built environment on the island. The reasons for the limited extent of damages despite the large acceleration levels and ground displacements that were recorded are primarily owing to the special confined-masonry system that was employed to construct buildings in the island following the widespread destruction of 1953. The lessons learned from the performance of this system are valuable and are the main subject of the present paper.

2   The 1953 earthquake

On the 9th of August of 1953, a series of strong ground motions begun, with epicenters located in the Ionian Islands. The strongest of all, having a magnitude of $M = 7.2$ and intensity of $X +$ on the Mercalli scale, occurred on August 12, with the epicenter located south of the island of Cephalonia (see green star in Fig. 1). This earthquake caused practically complete destruction of the building stock in the neighbouring islands of Zakynthos, Ithaca as well as on Cephalonia. Note that at the time, buildings were already partially damaged due to the many shocks that preceded the main event. Of a total number of 33000 buildings, 27659 buildings collapsed, whereas 467 buildings in the northern part of Cephalonia remained almost intact. The rest of the buildings that did not collapse developed extensive damages. In total 455 people were killed, 21 were reported missing, and 2412 were injured. 145000 residents were left homeless. Fig. 3 depicts a photo of Argostoli in Cephalonia after the earthquake.

The buildings of Cephalonia were for the most part two storey load-bearing masonry structures whereas several three storey buildings were not uncommon. A significant number of rural buildings were adobe constructions; in his historical documentary titled "How did our houses collapse", Pavlatos [11] attributes these collapses to (a) the age of the structures, (b) their old-fashioned methods of construction, and (c) the compounded damage owing to previous seismic events. However, a significant contribution to their vulnerability was owing to the inadequate morphology of their structural system, comprising only perimeter load bearing walls, very flexible floors (lacking any diaphragm action), the heavy timber roof and often, the heavy marble slabs that were supported on the walls through cantilevering beams or corbels. Although rules were already in place for earthquake–resistant construction based on the notions of the time and proposed after the devastating earthquake in Corinth on 1928, these rules had not been followed in Cephalonia. Nevertheless, three buildings that had been constructed compliant to these requirements in Zakynthos survived the earthquake with no damage.
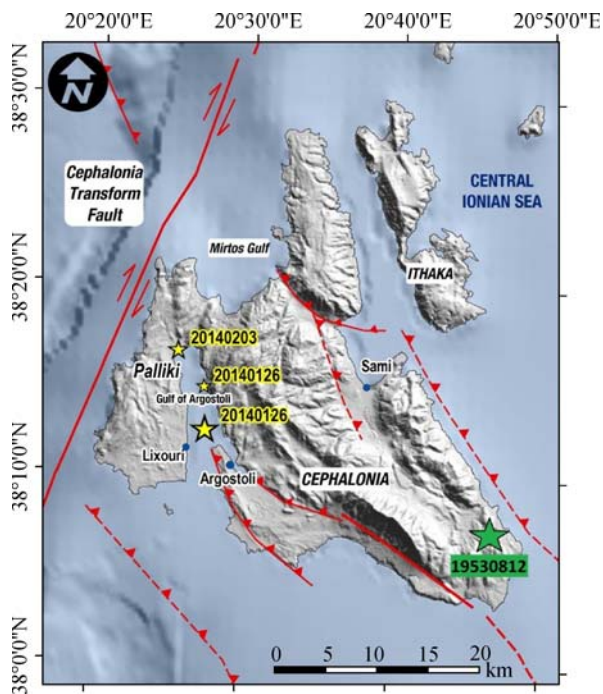
Fig. 2 Seismic damage due to the 2014 Cephalonia Eartquake, (a) and (b) recently constructed R.C. buildings with notable deficiencies non-conforming to the established code practices, (c) and (d) in URM buildings built prior to the big earthquake of 1953

Fig. 3 The town of Argostoli, capital of Cephalonia, after the 12/8/1953 earthquake

As mentioned in the preceding, 145000 inhabitants were left homeless – to address the pressing need for emergency housing, during the decade that followed the earthquake, the Ministry of Public Works funded the construction of 27394 small houses. Most of those were built according with prototype designs that included architectural drawings, full structural blueprints and construction details. The developed system could be classified today under "confined masonry construction" as detailed in Section 3. As the money were provided through Government Aid (Aid = Arogi in Greek) these buildings became later known as "Arogi houses."

The 2014 earthquake series did not cause any damage to these buildings, provided they were still in their original state (no architectural or structural alterations). Damages were observed only to such buildings that were modified from the original state through additions and extensions. It is likely that improper interventions as well as the use of non-compatible structural systems e.g. reinforced concrete frames combined with load bearing walls, were the cause for the damage. The excellent seismic performance of the Arogi buildings under the excessively high accelerations recorded in the 2014 event was the motivation behind the present investigation aiming toward improved understanding of their function as a structural system.

3 The Arogi buildings: description

The Arogi buildings in Cephalonia were primarily built in the villages around the urban areas of Argostoli and Lixouri (Fig. 1). The structural system is a combination of reinforced masonry and confined masonry and may be classified as confined masonry (CM) because the bed-joint

reinforcement is rather a wire than rebars. In more details: reinforcement is placed along the horizontal beds and is anchored in the vertical zones of reinforced concrete which are constructed at the intersection between load bearing elements. A perimeter reinforced concrete beam is also placed at the crest of all the walls. Wall piers having a length that exceeded 2.00 m were reinforced with vertical bars. Details are provided in the following section. The wall materials available for the project were (a) concrete blocks made specifically for this class of structures, with a relatively high content of cement so as to secure a high concrete strength (see Section 4 for estimated material properties), (b) fired clay bricks. From field observation, it is concluded that most users opted for the former (concrete blocks). The state organization overseeing the construction provided drawings for different plan sizes considering the needs of each family. The façade was placed according with the orientation of the plot. The prints of two typical plan drawings are depicted in Fig. 4; storey height is 2.7 m, top of the roof is at 4.0 m. As stated earlier the design drawings included façade views, sections, and detailing drawings that included information on the placement of reinforcement in plan and in height, in the pilasters and the top beam, as well as in footings. From the drawings, it is concluded that interior dividing walls also have a footing and they are connected through horizontal reinforcement with the primary load bearing walls.

3.1 Structural details

The structural drawings of the one storey building of Fig. 4(b) were found for both types of materials considered, i.e., concrete blocks and of clay bricks. According to verbal records the two-storey houses comprise three-wythe masonry; the outer wythes are of solid clay bricks whereas the middle layer is of reinforced concrete. However the type of masonry used in one-storey building construction is considered in the remainder of the present work for the sake of comparison but also as site evidence indicates that this type was used for construction of the majority of two storey houses also. The floor of the second storey is a reinforced concrete slab. In the following, details are presented for two types of buildings as it is concluded from the original drawings of 1954. An unfinished structure of this type is depicted in Fig. 5. Due to their structural system and the combination of reinforced concrete that is cast on pre-constructed masonry walls, these buildings qualify as Confined Masonry structures (http://www.confinedmasonry.org/). Performance of confined masonry buildings in past strong earthquakes illustrates favorable performance with minimal damage and well distributed cracking, owing to the redundancy of the lateral load system created by the network of perimeter reinforced concrete elements cast integrally with all masonry walls [12–15].

3.1.1 Concrete-block masonry one-storey houses

Wall thickness is 0.25 m comprising a single wythe concrete masonry (CMU) with block dimensions ($l \times h \times w$) $340 \times 250 \times 140$ mm produced especially for the restructuring project in the Ionian Island. Each block had two vertical openings accounting for 30% of the horizontal section of the masonry unit. Horizontal (longitudinal) reinforcement was placed in the middle of the wall thickness described as $\phi 4/15$, thus a 4 mm diameter bar is placed in each horizontal bed, Fig. 7. In the windowsills a single reinforcing bar 12 mm diameter ($1\phi 12$) runs through the entire length of the wall. Bars are anchored in the reinforced concrete zones which occur at the intersection of walls and in the corners. The openings are bounded by pilasters of length ranging between 4 and 10 cm, reinforced with vertical bars ($1\phi 12$) as shown at the top of Fig. 6. In the case of piers longer than 2 m, a vertical bar having a diameter of $\phi 10$ is placed at mid-length, placed internal to the longitudinal bars. Masonry is confined by reinforced concrete zones having a range of sizes (see for example Fig. 8 for the building of Fig. 4). Vertical bars in these zones are $4\phi 12$ in the corners and $4\phi 8$ in the other cases. Dividing clay brick walls having a thickness of 0.10 m were reinforced with a single 3 mm diameter wire in each bed. These bars were bent into the beds of intersecting walls thus connecting the dividing walls with the load bearing ones. Horizontal zones of reinforced concrete which served as the perimeter lintel were reinforced with $3\phi 12$ bottom, $3\phi 10$ top, and one $\phi 4$ at mid-depth. Stirrups were required according with the drawings only over the openings ($\phi 4$ at a spacing of 100 mm). However, it was observed that stirrups had been placed over the length of the wall. Fig. 6 shows details of a wall in elevation and of a horizontal section and Fig. 7 shows a vertical section of the wall with the necessary lintel and foundation details. The plinth is 0.40 m wide and about 0.50 m in height, depending on ground condition; $2\phi 12 + 1\phi 10$ bars are placed in the upper face, $3\phi 12$ bars are placed in the bottom and $1\phi 10$ rebar is encased at mid-height. The slab of the ground floor is supported by the plinth and resting on the ground. The foundation strip has 0.50 m width and about 0.50 m height depending on soil conditions and is of unreinforced concrete. Gravel is filling the excavation around the foundation in order to absorb the seismic motion. Figures 9 and 10 depict an unfinished building where the details of the lintel and pilasters are evident.

3.1.2 Buildings constructed of fired clay bricks

Wall thickness was 0.24 m and comprised two wythes of solid bricks. The horizontal reinforcement ($\phi 4$) was placed every second bed joint of each wythe, so that at least one bar would be provided within each bed: thus the reinforcement corresponding in each wythe would be a
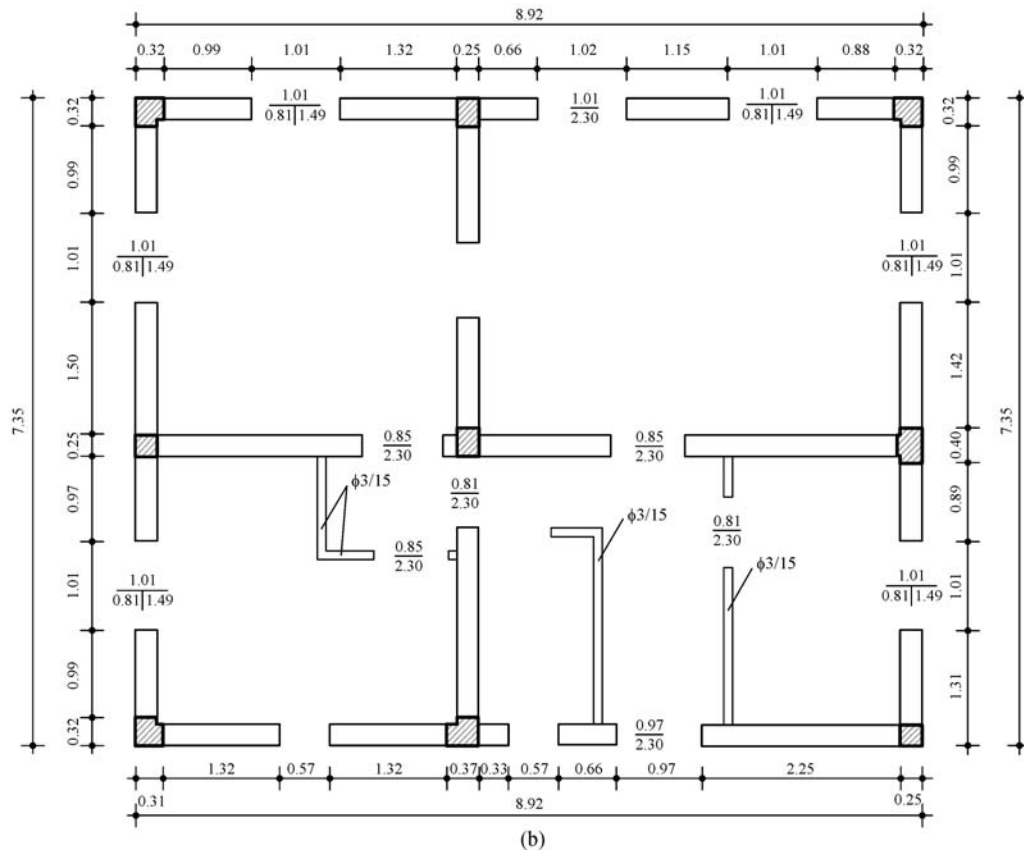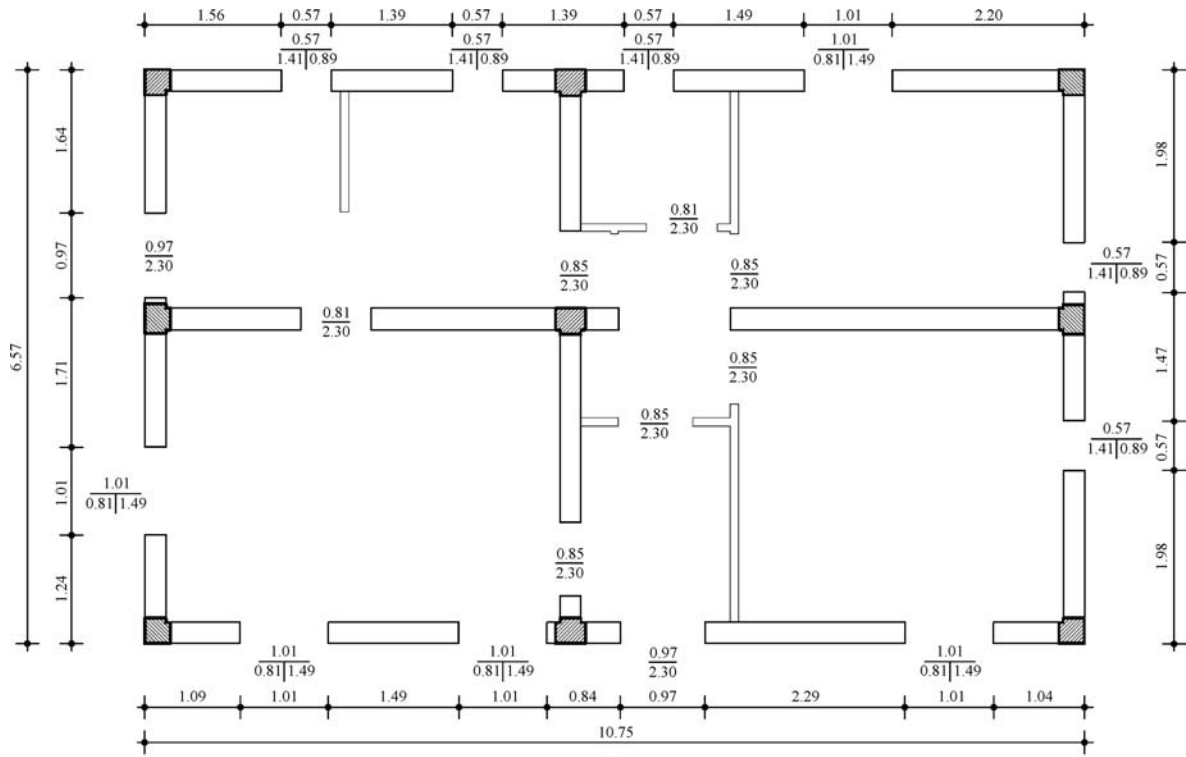
Fig. 4 Typical plans of two Arogi houses. (a) 70.63 m^2; (b) 65.65 m^2
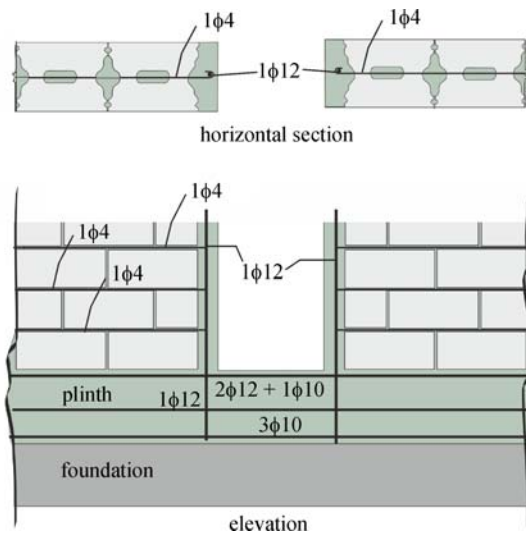
Fig. 5   An unfinished brick CM

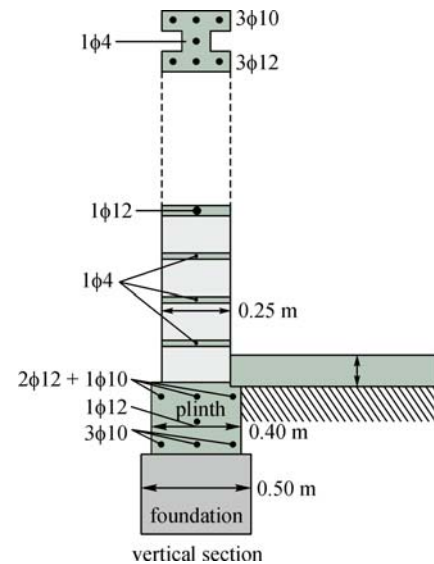**Fig. 6**   Reinforcing detail in the pilasters

Fig. 7   Vertical section of a wall of concrete units

4 mm diameter bar every 200 mm (ϕ4/200). The corner confining zones were 0.24×0.24 m reinforced with 4ϕ12. The intermediate confining zones were either 0.24×0.24 or 0.24×0.30, reinforced with 4ϕ8. Lintels contained 2ϕ14 top and an equal amount of bottom reinforcement. All other details were as in the case of buildings made of concrete blocks. In Fig. 11 the reinforcement of the two buildings of Fig. 4 is depicted.

3.2   Seismic performance of the Arogi buildings.

Buildings were constructed initially according with the guidelines provided, but later they underwent various alterations. These consisted of height-wise extension by the occasional addition of a floor, or laterally with the addition of extra spaces. As time passed attenuating the memories from the destruction caused by the 1953 earthquake, the urgency and need for seismic protection was downgraded in terms of momentum and commitment. Thus, in some cases, the additions comprised primarily of URM with voided brittle clay bricks; a frequent occurrence was the extension to comprise of a reinforced concrete frame.
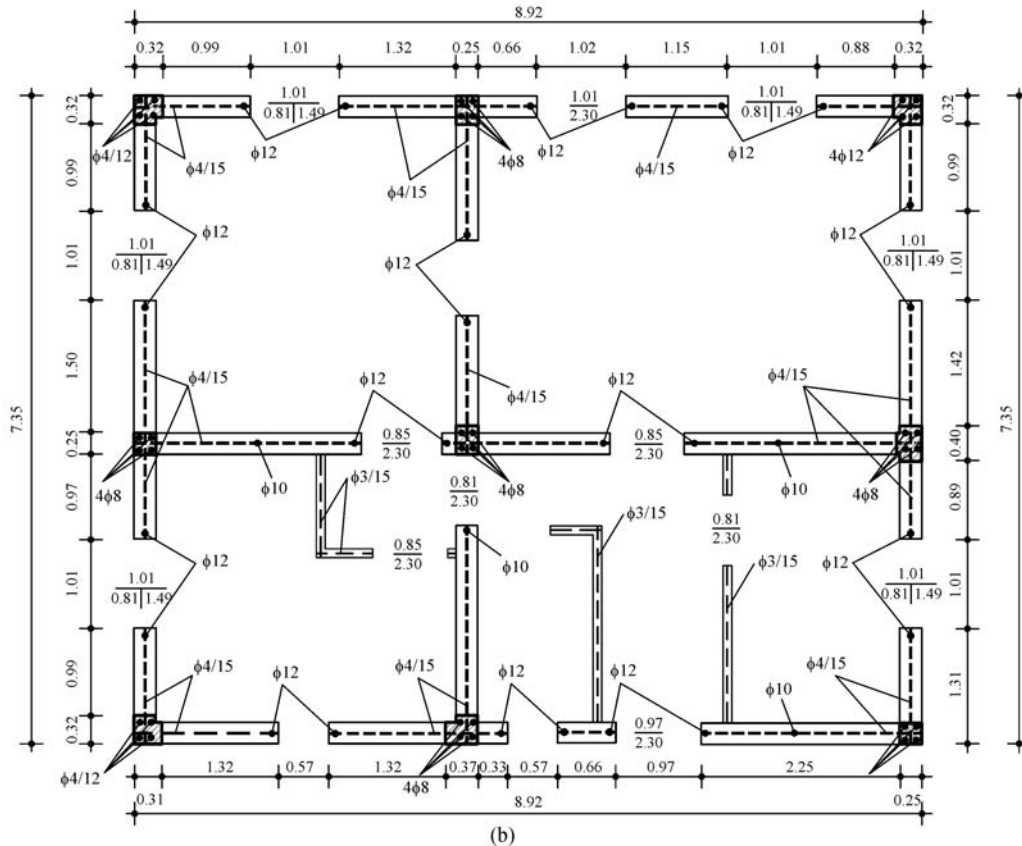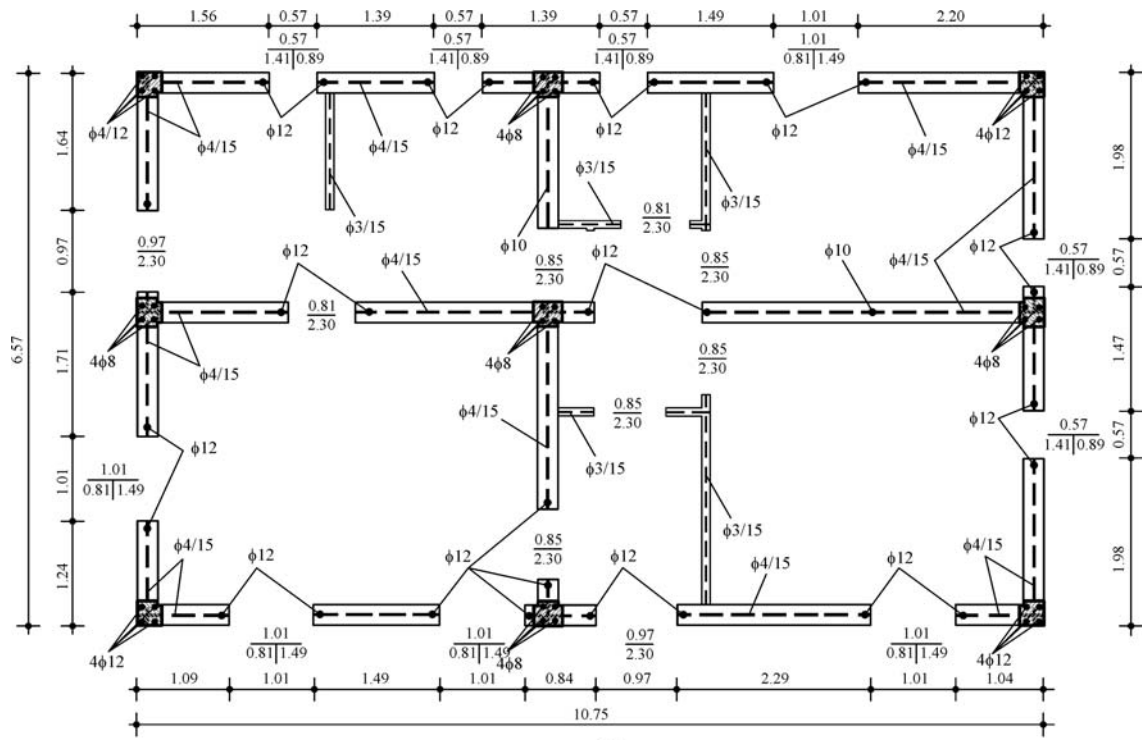
Fig. 8 Structural print with plan view of the buildings of concrete units masonry depicted in Fig. 4

Fig. 9 A wall comprising concrete-block masonry. Note the arrangement of the lintel beam

Fig. 10 In the entrance corner of the semi-complete house note the vertical reinforcement as well as the starter bars for lap splicing reinforcement of the second floor at the crest of the first floor perimeter beam

From the reconnaissance reports it was found that the original Arogi-buildings that had not sustained systemic alterations through additions performed very well although the ground acceleration was the highest ever recorded (0.76 g horizontally and 0.51 g vertically); buildings showed no signs of damage, even in the outside veneers. Some abandoned buildings showed damage in the roof owing to the strong vertical component of the ground motion. Figure 12(a) shows an Arogi-building in its original state, and Fig. 12(b) shows an identical structure with a lateral extension. Both buildings are photographed immediately after the 2014 earthquake, and no damage is reported in either case. However, the additions sustained extensive damages, whereas the damage to the supporting original structure ranged in intensity from light to very serious (Fig. 13).

An earthquake event of the scale that occurred in the 2014 earthquake in Cephalonia is a rare field test for the existing building stock. The good seismic performance of the Arogi buildings during the 2014 earthquake motivated the authors to further investigate their behavior through parametric analysis. The objective is to compare the seismic demand – expressed in terms of relative drift ratios, which quantifies the deformation of the Arogi buildings which are a type of CM construction, with the demands under the same earthquake occurring in traditional unreinforced stone masonry buildings (URM) that is a common building type throughout Greece. Also of interest is comparison of demands with those arising in buildings that comprise plain masonry in the context of EN1996-1-1:2005, namely, unreinforced masonry buildings with a reinforced concrete tie beam at the top of each floor; note that EN1998-1 demands the construction of rigid floors and roof cast integrally with the tie-beams. The effect of the selected type of diaphragm is also examined (reinforced concrete slab as compared with a flexible timber roof). In the parametric investigation conducted, single storey and two storey buildings were considered; thus in total, the following 12 types of buildings shown in Table 1 were assessed analytically, all having the same plan view.

For each case the calculated seismic demand is reported. In addition, the maximum value of a failure criterion that estimates the wall area ratio where the calculated elastic stresses (and associated strains) exceed the failure limit are compared for the cases examined (Karantoni et al. [16], see section 0 for a detailed review of the criterion used).

4 Assumptions of the parametric study

The earthquake may be considered as an experiment at full scale; the 2014 earthquake in Cephalonia proof-tested the confined masonry system used in the reconstruction of the islands after the devastating earthquakes of 1953. As the objective of this paper was to investigate the performance of the buildings if the traditional masonry construction had been used instead, a plan design was chosen for which all the construction details were available in (Fig. 4(b)) corresponding to the building depicted in Fig. 12(a). For the analysis of the 12 cases described in the preceding section, the following assumptions regarding the materials and loads were made.

In modeling the Arogi-building the walls' material modeled comprised concrete blocks as this was the most common choice in the field. In light of the relatively low area represented by the voids provided for passage of reinforcement, these building blocks are classified in group 2 according with EN 1996-1-1 [17]. Conservatively the compressive strength of masonry units f_{bc} was taken equal to 15 MPa. Since cement-lime mortar was used in the bed joints, a compressive strength f_m equal to 2.5 MPa was used. For the dimensions of concrete masonry units, the modification factor according to EN 772-1 to EN 772-6 is
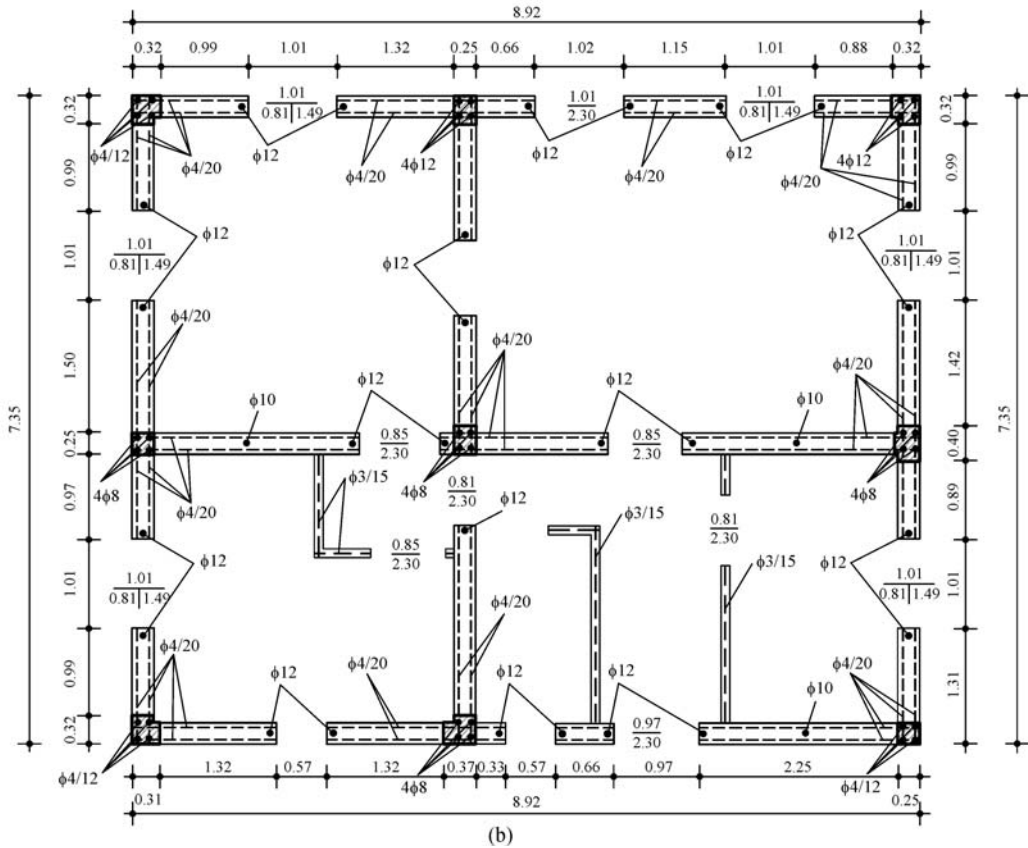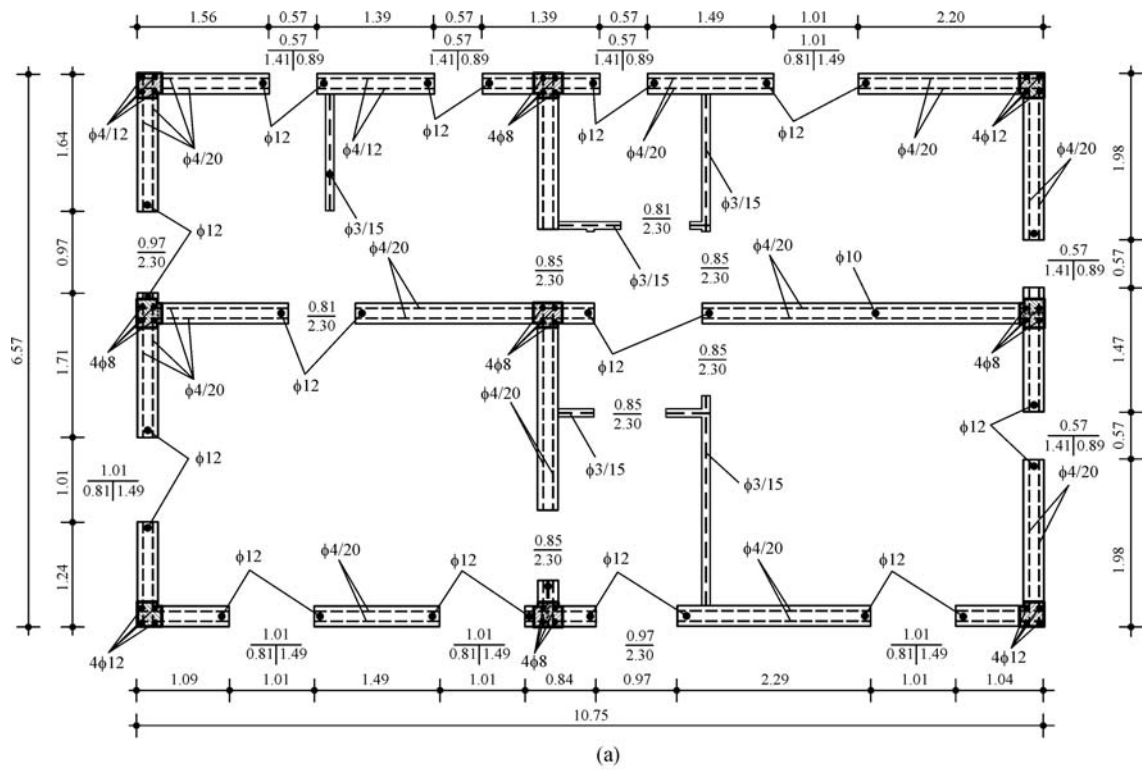
Fig. 11   Structural print, plan view of buildings of Fig. 4 of clay brick masonry units

(a)

(b)

Fig. 12 Two "Arogi Houses" - condition of both as was after the earthquake. (a) As built (b) with lateral extension to the left, through a URM addition

Fig. 13 Extension in height with the addition of a reinforced concrete frame

$\delta \approx 0.95$, thus the compressive strength of masonry according to Annex E of EN 1998-3:2020:E [18], calculated from Eq. (1) is 4.22 MPa.

$$f_w = 0.50*(\delta*f_{bc})^{0.70}*f_m^{0.30}. \qquad (1)$$

The elastic modulus of masonry is approximated as E = $1000f_w$ = 4200 MPa, but in the present analysis an effective elastic modulus $E_{\text{eff}} = 0.5E$ = 2100 MPa was taken, in order to account for cracking and aging. For the sake of comparison, the same mechanical properties were assumed for the URM stone buildings. The self-weight of masonry was taken equal to 22 kN/m³. The concrete was considered as B10 class (with compressive strength of a cube equal to 10 N/mm²). It is worth mentioning that in the era under consideration the contents of the concrete mixture were pre-described to achieve the favorable compressive strength. For the calculation of the seismic loads in the parametric investigation the strong ground motion with the highest possible acceleration was used; these were recorded from a relatively dense network of accelerographs which was enhanced further after the first seismic event. Records used are from the 03/02/2014 event in the Chavriata area of Cephalonia (http://www.itsak.gr/db/data). Figures 14 and 15 plot the pseudo-acceleration response spectra along the E-W (East–West), N-S (North–South) and U-D (Up-Down) directions for damping ratios of 5%, 10% and 20% and the associated relative displacement spectra. At low periods (0.25 s) the spectral acceleration (Sa) reached 2.9 g (N-S component), while at periods near 0.75 s, Sa was in the range of 1.5g (Fig. 14). In the E-W component spectral accelerations reached 2.7 g (T = 0.25 s) and 0.8g (T = 0.75 s), respectively. Those high values are due to the short distance from the hypocenter to the recording station. Note that the recorded peak ground acceleration (estimated from the coordinate at the left of the pseudo-acceleration spectrum of Fig. 14 for period tending to zero for 5% damping ratio) was, α_g = 0.76 g, as in Theodoulidis et al. [19]. As shown in Fig. 15, in the short period range spectral relative displacement values are less than 5 cm, but increase gradually for longer periods (up to 3 s). A convergence of all three orthogonal components (displacement plateau) is observed at T = 2.5 s.

5 Modeling of structures and load effects

Buildings were modeled in 3-D using finite elements while accounting for both the in-plane and out-of-plane response of the masonry walls (isoparametric shell elements with 6 d.o.f. per node). The elements were triangular or quadrilateral (with 3 or 4 nodes each, respectively), depending on the distribution of the nodes which also depends on the location of the windows and the doors; the used program code ACORD-expert (http://www.itech-bois.com/fr/Telechargement/log/ACORD-Expert/ACORD-Expert.htm) selects the type in order that the mesh may be optimized. The thickness of the finite elements was set equal to the wall thickness while the average mesh size was

Table 1 Cases studied in parametric investigation

building type	sumber of stories	floor type	roof type	case ID
Arogi-house (concrete block masonry)	1	-	timber	CM-1T *
	1	-	R.C. slab	CM-1S
	2	timber	timber	CM-2TT
	2	R.C. slab	timber	CM-2ST
			R.C. slab	CM-2SS
stone URM	1	-	timber	URM-1T
	1	-	R.C. slab	URM-1S
	2	timber	timber	URM-2TT
	2	R.C. slab	timber	URM-2ST
			R.C. slab	URM-2SS
plain masonry	1	-	timber	PM-1T
	2	timber	timber	PM-2TT

* t = timber
S = reinforced concrete slabs
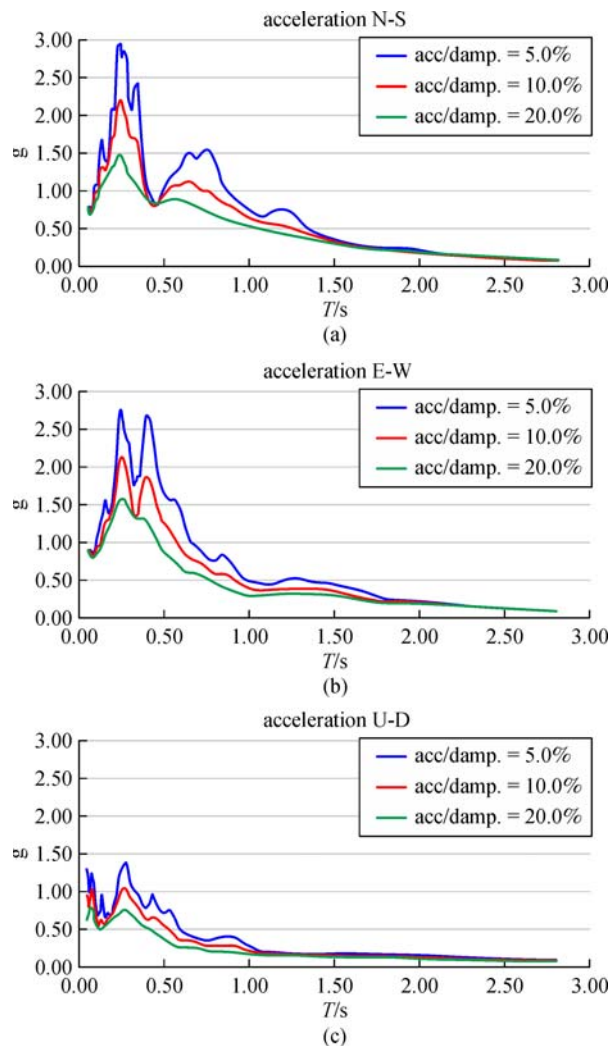
Fig. 14 Acceleration response spectra of the strong ground motion recorded in the Chavriata Station on 03/02/2014 (in g)

about 0.50×0.50 m depending upon the dimensions of piers and openings; finite elements modeling the tie zones were set equal to the dimensions of those zones. The finite elements were assigned the material properties of the region they model, namely reinforced concrete or masonry. Typical building models studied herein and the corresponding finite element discretization of the structures are shown in Fig. 16. Gravity loads from the timber roof were transferred to the walls as axial compression. The analysis was performed under static lateral loads resulting from a uniform distribution of lateral acceleration along the building height, $S(a) = 1.0$ g (i.e., acceleration equal to that of gravity, applied however in the lateral direction along the principal axes x and y of the building). As shown in Fig. 14 this acceleration level is the value from the total acceleration response spectrum of the earthquake considered, that corresponds to periods less than 0.1 sec. The underlying concept of this approach may be traced to Rayleigh's method of approximation [20], and EN-8-1, Annex B [18]. According with this approximate method, the structure is modeled as a generalized single degree of freedom, where the fundamental response shape is evaluated as the displaced shape assumed by the structure when it is loaded laterally with a gravitational field. It is relevant to note here that this is the anticipated range of structural periods for the buildings analyzed [21,22]. The response acceleration value $S(a)$ remained the same in all the cases studied so as to enable immediate comparison. In the narrow range of variation of the fundamental periods of the 12 different buildings (0.05–0.09 s) and given the uncertainty in its estimation this approximation was considered realistic. Applying a field of accelerations rather than nodal forces is more appropriate when continuous systems are examined (such as masonry) as in this manner all masses are engaged proportionally without the requirement of calculating nodal forces which in structures with
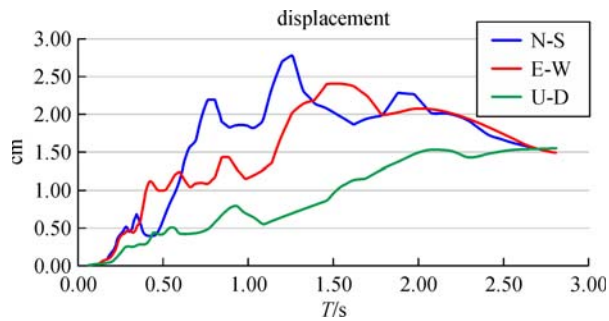
Fig. 15 Displacement response spectra (for 5% damping) of the strong ground motion recorded in the Chavriata Station on 03/02/2014 (in cm)

distributed mass could be an onerous task (see Pardalopoulos et al. [23]). The analyses were conducted for the seismic combinations $G + 0.3Q + E_x + E_y$ and $G + 0.3Q + E_x + E_y \pm E_z$ in order to also consider the effects of the high value of the vertical component (Fig. 14). The live load Q was taken 2 kN/m^2. The field of nonlinear Finite Element analysis of unreinforced or lightly reinforced masonry structures is hampered by several issues related to stability and convergence of the algorithm in the absence of robustness in the stiffness matrix after cracking even of few elements. To circumvent this difficulty various alternative approaches are considered in the literature; those include the use of macroele-

Fig. 16   Idealized buildings studied parametrically and corresponding finite element discretization

ments which represent the behavior of entire walls and spandrel components using nonlinear truss panels [24], but also modification of linear elastic analysis results (through μ-q-T relationships) to estimate the inelastic demands from the corresponding elastic values. The latter approach is pursued here for the sake of simplicity. Herein results are given for the combination $G + Q + E_x + E_y$ with reference to four different parameters: (a) Peak displacement of the most displaced node in the structure, (b) Relative displacement of the most displaced node with respect to the base of the diaphragm immediately below (lying on the same vertical line), divided by the vertical distance between these two points of reference; this is the interstorey drift ratio denoted henceforth by d_h, (c) Relative displacement of the same point, with reference to the least displaced node in the same horizontal level that belongs to the same member (wall or pier), divided by the horizontal distance between the two points (horizontal drift ratio due to out-of-plane action), denoted as d_{pl}, and (d) The value of the failure criterion for the masonry walls which quantifies the surface area where stresses exceed the plasticity limit; the criterion was established earlier by Karantoni et al. [16] and is described in detail in the following section.

6 Criterion for masonry wall failure

In conducting the simulations, a plasticity-based isotropic constitutive model was used to evaluate the stress-strain behavior of stone-masonry walls under plane stress (i.e., for post-analysis assessment). Considering that the material is taken as linear elastic up to tension cracking or compression cracking, attainment of the failure envelope by a stress state implies that the state of strain has also attained the corresponding cracking limits. Several alternative biaxial failure envelopes have been used to quantify the damage accumulated in the semi-brittle and tension-deficient material under plane stress (e.g., Refs. [25–29], among others). A relevant model was developed by the author to quantify the extent and intensity of material failure [16]. The model was obtained after calibration of a well-established four-parameter failure envelope (Otto-sen's criteria intended for semi-brittle materials), with a large database of biaxial tests conducted on brick masonry wallettes. Parameter of study in this calibration was the angle forming between the directions of principal tension and that of the masonry bed joints. Here the failure envelope for masonry under a triaxial stress state is [30]:

$$a\frac{J_2}{f_w^2} + \lambda\frac{\sqrt{J_2}}{f_w} + \beta\frac{I_1}{f_w} = 1. \qquad (2)$$

Parameters I_1 and J_2 are the first invariant and the second deviatoric stress invariant of the stress tensor at any point in the material domain. Parameter λ depends on the inclination of the octahedral plane, θ :

$$\lambda = c_1\cos\frac{\cos^{-1}(c_2\cos3\theta)}{3}, \text{ if } \cos3\theta \geqslant 0, \qquad (3)$$

$$\lambda = c_1\cos\frac{\pi - \cos^{-1}(-c_2\cos3\theta)}{3}, \text{ if } \cos3\theta < 0, \qquad (4)$$

where,

$$\cos3\theta = \frac{3\sqrt{3}\,J_3}{2J_2^{3/2}}. \qquad (5)$$

Note that $\theta = 60°$ for uniaxial compression, $\theta = 0°$ for both uniaxial tension and biaxial compression, and J_3 is the third deviatoric stress invariant. Also,

$$\beta = \frac{1}{3}\left(\frac{1}{f} - \frac{1}{b} + \frac{b-f}{3}a\right). \qquad (6)$$

Parameter α in Eqs. (2) and 6 is a function of the stress condition and f is the ratio of tensile to compressive strength of masonry, whereas b is the strength ratio under symmetric biaxial compression; best-fit calibration with the available experimental database [25,26] was obtained for $b = 1.65$ and $f = 0.085$. The failure envelope of Fig. 17 is constructed for $c_2 = 0.959$ and the obtained values calculated using, $\alpha = 0.665$, $\beta = 3.84$ and $c_1 = 13.8$ [16].
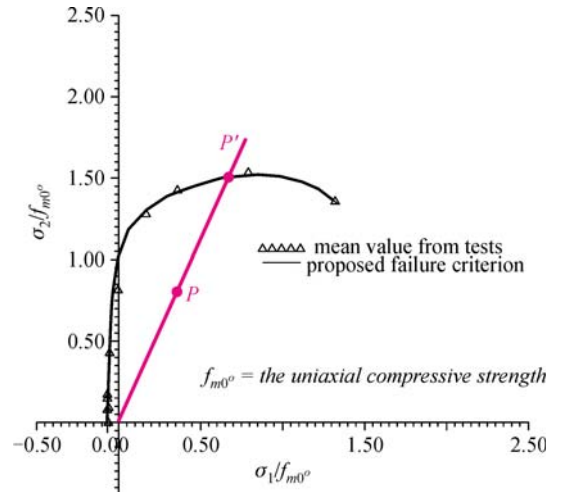

Fig. 17 The basis of the proposed failure criterion

Thus, in the stress space defined by the two orthogonal principal stress axes, an arbitrary stress state having stress coordinates σ_1, σ_2, is represented by the point P (Fig. 17). his stress state is evaluated with respect the failure envelope by considering the length of the radius OP', going through P, to the failure envelope to point P'. Denoting the ratio OP/OP' by σ^*, then, it is possible after normalizing the stresses σ_1 and σ_2 by σ^* to produce a stress state, σ_1/σ^*, σ_2/σ^* that lies exactly on the failure envelope. (Thus, the pair (σ_1/σ^*, σ_2/σ^*) satisfies the equation of the criterion Eq. (2)). In this light, practically
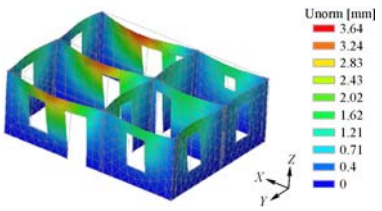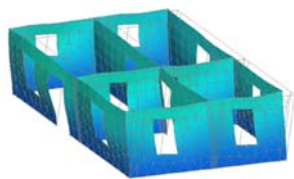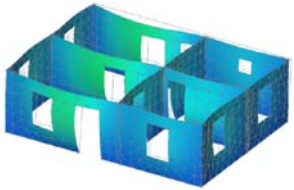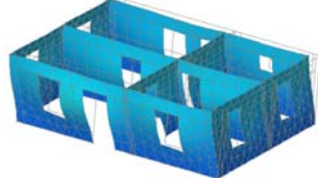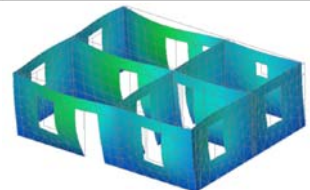
σ^* may be seen as a safety factor determining the proximity of the stress state to the failure envelope; it may be also considered as an extension of the concepts of a behavior factor $q = \sigma^*$ and the associated deformation ductility, $\mu = q = \sigma^*$, to a two-dimensional state of stress and strain. Thus, stress combinations values with $\mu = q = \sigma^* < 1$ lie inside the failure envelope, whereas cases having $\mu = q = \sigma^* > 1$ have reached plastification, which, in masonry is associated conceptually with failure due to the apparent brittleness of the material. Of course a wall does not really get damaged if only a single point exceeds the failure limit; the extent of damage is significant as an indicator of damage. To quantify the intensity of damage, the area ratio over a wall where $\sigma^* > 1$ is used as a meaningful index of damage in the present study.

7 Comparison of behavior of single storey buildings

Table 2 presents the deformed shape of the single storey buildings and the peak displacement attained; also, listed below is the reduction of peak displacement in relation to the corresponding value observed in building URM-1T (this is the traditional stone unreinforced masonry construction without lacing). Also provided are the values of the relative drift ratios described above, d_{pl} and d_h. From the information listed it follows that:

Using the confined masonry with timber roof (CM-1T) (e.g., Arogi Houses) caused a reduction of peak displacement from 3.64 mm to 1.30 (a 64% reduction from the value that would have occurred in traditional stone

Table 2 Distribution of displacement and drifts of 1-storey buildings for $G + E_x + E_y$

building	deformed shape	peak displacement % reduction	$d_{pl}/\%$ reduction	$d_h/\%$ reduction
URM-1T		3.64 mm reference value	0.14 reference value	0.13 reference value
UMR-1S		0.93 mm 74%	0.01 92%	0.03 77%
CM-1T		1.3 mm 64%	0.04 70%	0.07 45%
CM-1S		0.6 mm 84%	0.004 97%	0.03 78%
PM-1T		1.53 mm 58%	0.05 64%	0.08 35%

masonry construction with timber roof, URM-1T). Peak values of the drift ratios d_h and d_{pl} were reduced by 70% and 45% respectively: the values for URM-1T were 0.14% and 0.13%, and were reduced to 0.04% and 0.07% respectively. Using a combination of confined masonry and a concrete slab (CM-1S) effects a significant reduction in displacement and drift ratios however also increasing the costs. From the 2014 field evidence, it is concluded that it was not necessary to increase the strength by such a high margin. In case a house of URM with concrete slabs (URM-1S) was used peak displacement was reduced by 74%, from a value of 3.64 to 0.93 mm however, in comparison with CM-1T, the required solution would still need a timber roof to be placed over the slab so as to avoid architectural alterations of the settlement, thereby increasing the cost disproportionately as compared with the improvement of performance, which is in the order of 10%. As was expected, the plain masonry building (PM-1T) performed better than the URM-1T, as evidenced by a 58% reduction in peak displacement and a 64% and 38% reduction in the value of the drift ratios d_h and d_{pl}, respectively. The results are compared with those of CM-1T mainly owing to the presence of the reinforced concrete tie beam. Thus, for one storey houses, the Arogi-Buildings comprising confined masonry were more than adequate to support the imposed demands. Confined masonry and reinforced concrete in the slabs was the solution that caused a most remarkable reduction in displacement at the expense of a significant increase in the cost of retrofitting.
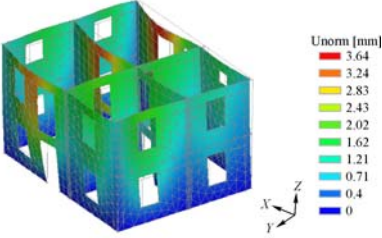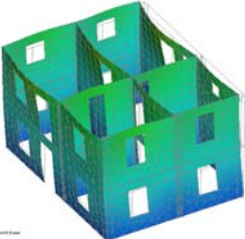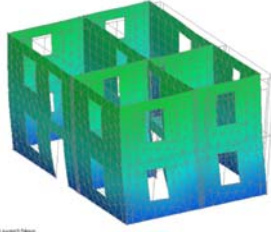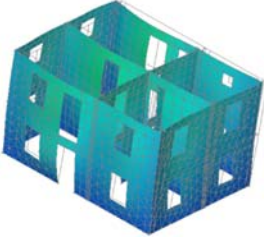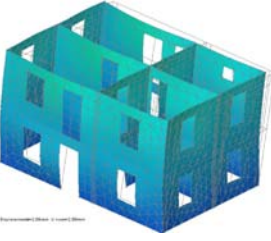
Similar behavioral trends were obtained when the modified Ottosen criterion described in the preceding was used to assess the vulnerability of the structures analyzed. Calculated results are listed in Table 3; values in red refer to the regions of the masonry where failure is anticipated (in this context failure is identified by stress states that lie outside the failure envelope (Fig. 17).) The overstressed areas are also provided (as an area fraction of the damaged over the total available wall area; the most critical value considering both facades is listed). Note that the zones of reinforced concrete are not shown in this representation; only masonry is considered. Specific findings are as follows: For the magnitude of recorded ground accelerations, no damage was observed in the "Arogi" buildings. This finding is consistent with the analysis results. For example, in building CM-1T (Table 3) the fraction of the masonry area marked in red is only 0.3%; this was estimated to be lower by 96% as compared to the case where URM had been used: in the URM case 8.6% of the wall area would be outside the failure envelope. Practically this damage level corresponds to "Damage Grade I" according with the European Macroseismic Scale, Grünthal [31]. Note that the most vulnerable parts of the walls are the lintels, as it is also shown in Table 2. Using a reinforced concrete slab as a diaphragm in the unreinforced masonry structure (URM-1S) reduced the

Table 3 Wall areas where failure criteria is exceeded
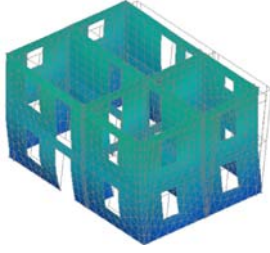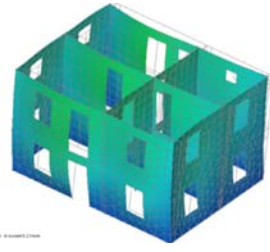
building ID	overstressed area percent reduction
URM-1T	8.6%
	reference value
URM-1S	2%
	78%
CM-1T	0.3%
	96%
CM-1S	0%
	100%
PM-1T	1%
	88%

intensity of demand in the building by 78%; this however was inferior to the mitigation level achieved through CM-1T which caused a reduction by 96% in the area of damaged region in the masonry walls. In plain masonry (PM-1T) the overstressed area represents 1% of the total area of masonry walls. This means the house remains practically unaffected by the earthquake. Last, but not least, the use of a slab on the "Arogi"-building (confined

Table 4 Distribution of displacement and drift ratios of 2-storey buildings for $G + E_x + E_y$

building	deformed shape	max displacement /mm % reduction from reference	d_{pl}/% % reduction from reference	d_h/% % reduction from reference
URM-2TT		8.25 mm ref. value	0.285 ref. value	0.18 ref. value
URM-2ST		5.6 mm 32%	0.156 45%	0.15 17%
URM-2SS		3.54 mm 57%	0.007 97%	0.03 81%
CM-2TT		2.64 mm 68%	0.066 77%	0.06 68%
CM-2ST		2.09 mm 75%	0.037 87%	0.08 74%

building	deformed shape	max displacement /mm % reduction from reference	$d_{pl}/\%$ % reduction from reference	$d_h/\%$ % reduction from reference
CM-2SS		2.05 mm 75%	0.003 99%	0.05 87%
PM-2TT		3.21 mm 61%	0.08 77%	0.08 68%

masonry, CM-1S) completely mitigated any occurrence of damage in the masonry structure.

Figure 18 depicts a comparison of the maximum displacements and values of the failure criterion obtained for the five cases of single storey buildings. It is shown in Fig. 18 (b), that in case URM-1T the criterion exceeds the value of 3, which means that the stress-state is three times higher than the strength, based on the selected criterion. To the contrary, the few points that lie outside the failure envelope in the case of the "Arogi" houses are relatively close to the limit since for those cases the values of the criterion are around 1.5. Note that the presence or not of a slab does not significantly affect the value of the criterion, and therefore the results confirm the decision to not build a slab in the one-storey houses of "Arogi." From Fig. 18(c) it is observed that in case of URM-1T most critical is the horizontal out-of-plane displacement, d_{pl}, whereas in all the other cases examined, the relative out of plane displacement in the heightwise direction (interstorey drift, d_h) is more critical.

8   Two-storey buildings

To examine the response of the two storey "Arogi" houses to the 2014 earthquakes several variants to the basic model were examined as depicted in Fig. 16. To enable direct comparison, the same plan arrangements and material properties were considered as in the corresponding one-storey examples. In Table 4, which is the extension of Table 2 to two storey structures, the deformed shape of the

two storey buildings, the peak displacement attained and the reduction of this displacement in relation to the corresponding value observed in building URM-2TT (this is the traditional stone unreinforced masonry construction without lacing) are presented (see the cell below the displacement for the respective reduction). The first case listed is used as a point of reference. In Figs. 19(a) and (b) the maximum displacement and the value of equivalent stress σ^* and in Fig. 19 (c) the values of drift ratios are presented for each case studied.

For the two storey buildings the findings of the parametric investigation are summarized as follows:

Using the confined masonry system with a timber roof (CM-2TT) (e.g., "Arogi" Houses) caused a reduction in peak displacement from 8.25 mm to 2.64 (68% reduction from the value that would have occurred in traditional stone masonry construction with a timber floor also featuring the same timber roof, URM-2TT). Peak values of the drift ratios d_{pl} and d_h were reduced by 77% and 68% respectively: the values for URM-2TT were 0.285% and 0.18%, and were reduced to 0.066% and 0.06% respectively — these levels are well below the cracking limit of masonry which is estimated to be in the order of 0.15–0.2%.

The peak displacement of URM-2TT which is 8.25 mm was reduced to 5.6 mm or by 32%, after the replacement of the timber floor by a reinforced concrete slab (URM-2ST) and the drift ratios d_{pl} and d_h (See Table 4) were reduced by 45% and 17% respectively. When both the floor and the roof were replaced with reinforced concrete slabs, URM-2SS, the improvement of the behavior of URM −2TT was

Table 5 Wall areas where failure criterion is exceeded in two-storey building models

ID	overstressed area percent reduction	ID	overstressed area percent reduction
URM-2TT	23% -	CM-2TT	2.6% 88.7%
URM-2ST	13% 43%	CM-2ST	2.4% 89.5%
URM-2SS	18% 21.7%	CM-2SS	3.14% 86.3%
PM-2TT	9.5% 59%		

much better because the drift ratios of the most displaced upper floor wall were reduced remarkably, by 97% and 81% respectively, for horizontal and heightwise drifts. The use of confined masonry with timber floor and roof (CM-2TT) caused a reduction in maximum displacement by almost the same amount as URM-2SS but relative drift ratios were reduced even further by an additional 10%. Clearly the used system required a higher initial cost however, mitigation of damage in future seismic events offsets the initial expense as it results in a much better behaved structural system. The replacement either of the timber floor or both the timber floor and timber roof by

rigid slabs with a diaphragm function causes further reductions in peak displacement and in the relative drift ratios but increases significant the construction cost.

The use of plain masonry (PM-2TT) - masonry with r.c tie belts at the top of each floor as suggested by EN 1996-1-1 was found more effective than URM-2TT as it reduces by 62% the displacement and 72% and 52% respectively the drift ratios d_{pl} and d_h. It is worth to mention that plain masonry is a good option for the two storey buildings as compared to the URM but by EN1988-1 must be combined with rigid floors.

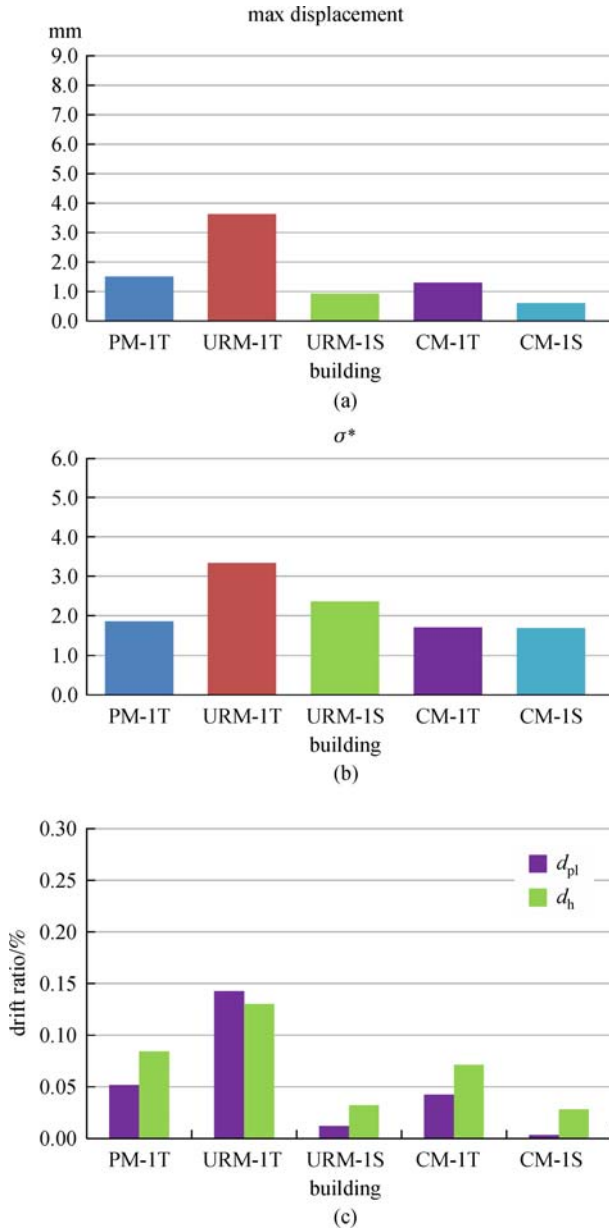Using the failure criterion of Section 6 to quantify the

Fig. 18 Max displacement (a) and failure criteria values (b) for one-storey buildings under $G + 0.3Q + E_x + E_y$; (c) comparison of relative drift ratios
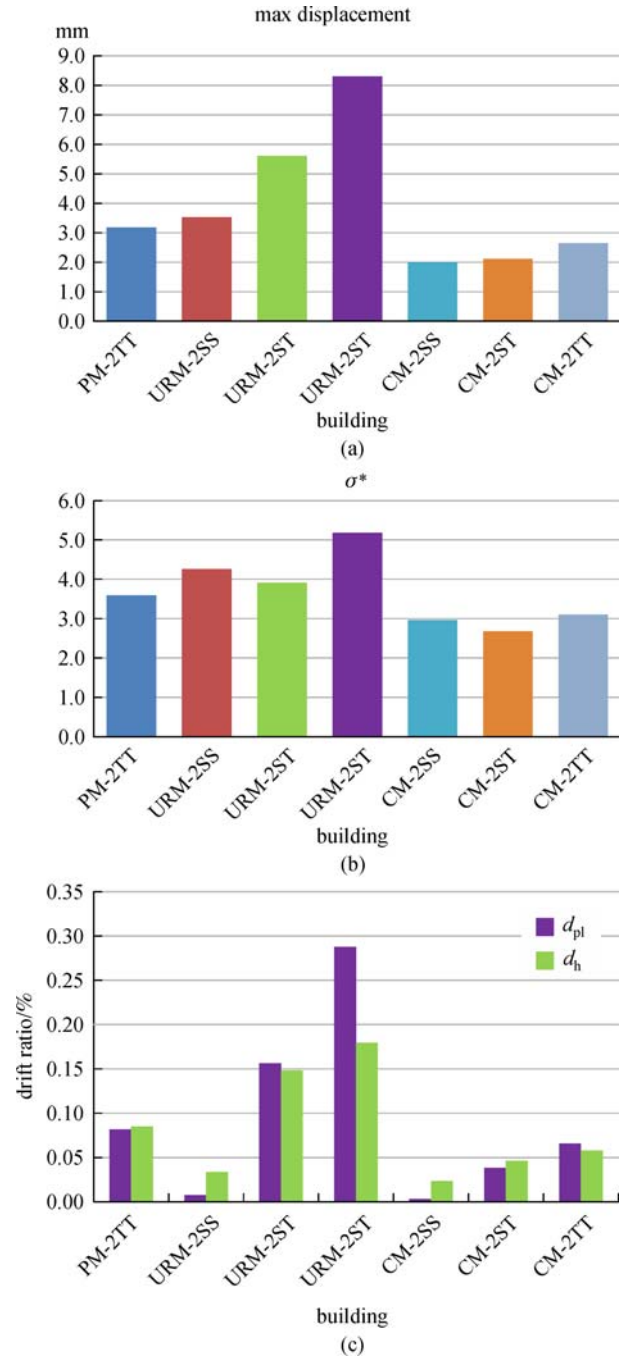

Fig. 19 Max displacement (a) and failure criteria values (b) for two-storey buildings under $G + 0.3Q + E_x + E_y$; (c) comparison of relative drift ratios

intensity of damage associated with the seismic demand, and taking into account that for the magnitude of recorded ground accelerations almost no damage was observed in the two storey "Arogi" buildings, this finding is consistent with the analysis results; for example, in building CM-2TT (Table 5) the fraction of the masonry area marked in red is only 2.6% and this would be by 88.7% lower than if URM-2TT had been used, in which case, 23% of the wall area would have stress-states that lie outside the failure envelope. Practically the damage level of URM-2TT corresponds to "Damage Grade 3" according with the European Macroseismic Scale [31] and it is reduced to

"Damage Grade 1" if CM-2TT is used [32]. Using a reinforced concrete slab as a diaphragm in the floor of first storey of unreinforced masonry structure (URM-2ST) reduces by 43% the intensity of demand in the building; this is however less than the mitigation achieved through CM-2TT.

Using a reinforced concrete slab as a diaphragm in the roof and the floor of first storey of the unreinforced

masonry structure (URM-2SS) reduced by 21.7% the intensity of demand in the building; this is however less than the mitigation achieved through CM-2TT which reduced by 88.7% the area of damaged region in masonry. It is noteworthy that the addition of one more diaphragm at the roof level is less effective in minimizing the extent of regions where the state of stress lies outside the failure envelope, as compared with the addition of a timber roof. The reason for this unexpected finding is that the weight of a concrete slab at that level increases significantly the base shear due to the increase in the system's mass (a heavier structure).

Addition of a slab in the Arogi Building (CM-2ST) practically did not improve the response since the fraction of the walls that are expected to fail is not affected (estimated at 2.4%) as compared with building (CM-2TT) where this fraction is 2.6%. The use of a slab instead of a timber roof is actually somewhat counter-effective exactly as was seen in the case of the URM buildings, since the areas that lie outside the failure envelope are in the order of 3.14% in building case CM-2SS.

9   Conclusions

From the analyses conducted it was shown that the use of confined masonry for the restructuring of the Ionian Islands following the devastating earthquakes of 1953 which wiped the building stock of the time, was an excellent choice. The selected building system demonstrated seismically resilient performance in the most severe seismic trial they have been subjected to since their construction, during the 2014 earthquake sequence.

The patent system of confined masonry devised for widespread use in reconstructing the destroyed island of Cephalonia after the devastating earthquakes of 1953 was tested during the 2014 strong ground motion that struck the area in near-fault conditions generating very high accelerations. Reconnaissance reports demonstrated that it is possible to build low-cost seismically-resistant masonry structures — a fact confirmed also through detailed parametric investigation for the types of structures studied [33]. Adding restraints to differential lateral displacements of diaphragms in successive floors was shown to be an effective means of strengthening in structures with two or more storeys. The significance of adding restraints was minimal only in one-storey structures due to the floor slab weight that causes an increase in inertia forces and base shear of the building. Seismic demand and assessment of structural condition were determined in terms of deformations or drift ratio, and by calculation of a failure criterion that relies on the area ratio of walls where the state of stress lies outside the failure envelope.

It is also relevant to note that the analysis conducted using uniform lateral accelerations equal to the total acceleration spectral value for structures having a period in the range appropriate for continuous masonry buildings produced results of equivalent accuracy with dynamic, step-by-step, dynamic analysis however it was very easy to conduct and in the processing of the output, enabling direct visualization of the effects of each parameter studied in the respective peak displacement, peak drift ratios and damaged area fraction (according to the criterion) in the structure.

References

1. Scordilis E M, Karakaisis G F, Karakostas B G, Panagiotopoulos D G, Comninakis P E, Papazachos B C. Evidence for Transform Faulting in the Ionian Sea: the Cephalonia Island Earthquake Sequence of 1983. Pure and Applied Geophysics, 1985, 123(3): 388–397

2. Louvari E, Kiratzi A A, Papazachos B C. The CTF and its extension to western Lefkada Island. Tectonophysics, 1999, 308: 223–236

3. Sachpazi M, Hirn A, Clément C, Haslinger F, Laigle M, Kissling E, Charvis P, Hello Y, Lépine J C, Sapin M, Ansorge J. Western Hellenic subduction and Cephalonia Transform: local earthquakes and plate transport and strain. Tectonophysics, 2000, 319(4): 301–319

4. Pérouse E, Chamot-Rooke N, Rabaute A, Briole P, Jouanne F, Georgiev I, Dimitrov D. Bridging onshore and offshore present-day kinematics of central and eastern Mediterranean: Implications for crustal dynamics and mantle flow. Geochemistry Geophysics Geosystems, 2012, 13(9): 371–387

5. Ganas A, Elias P, Bozionelos G, Papathanassiou G, Avallone A, Papastergios A, Valkaniotis S, Parcharidis I, Briole P. Coseismic deformation, field observations and seismic fault of the 17 November 2015 M = 6.5, Lefkada Island, Greece earthquake. Tectonophysics, 2016, 687: 210–222

6. Papaioannou Chr. Report of Institute of Engineering Seismology and Earthquake EngineeringResearch and Technical Institute, Strong Ground Motion Of The February 3, 2014 (in Greek)

7. Karastathis V K, Mouzakiotis E, Ganas A, Papadopoulos G A. High-precision relocation of seismic sequences above a dipping Moho: the case of the January–February 2014 seismic sequence on Cephalonia island (Greece). Solid Earth, 2015, 6(1): 173–184

8. Boncori M J P, Papoutsis I, Pezzo G, Tolomei C, Atzori S, Ganas A, Karastathis V, Salvi S, Kontoes C, Antonioli A. 2015, The February 2014 Cephalonia Earthquake (Greece): 3D Deformation Field and Source Modeling from Multiple SAR Techniques. Seismological Research Letters, 2015, 86(1): 124–137

9. Valkaniotis S, Ganas A, Papathanassiou G, Papanikolaou M. Field observations of geological effects triggered by the January–February 2014 Cephalonia (Ionian Sea, Greece) earthquakes. Tectonophysics, 2014, 630: 150–157

10. Papathanassiou G, Ganas A, Valkaniotis S. Recurrent liquefaction-induced failures triggered by 2014 Cephalonia, Greece earthquakes: Spatial distribution and quantitative analysis of liquefaction potential. Engineering Geology, 2016, 200: 18–30

11. Pavlatos D. 1988, *Coram Populo*, Editor Municipality of Argostoli, Greece

12. Tomaževič M, Klemenc I. Seismic behaviour of confined masonry walls. Earthquake Engineering & Structural Dynamics, 1997, 26 (10): 1059–1071

13. Astroza M, Moroni O, Salinas C. Seismic behavior qualification methodology for confined masonry buildings. In: Proceedings of the 12th World Conference on Earthquake Engineering, 2000, 1123–1124

14. Astroza M, Moroni O, Brzev S, Tanner J. Seismic performance of engineered masonry buildings in the 2010 Maule Earthquake. Earthquake Spectra, 2012, 28(S1 No. S1): S385–S406

15. Brzev S N. Earthquake-resistant confined masonry construction, national information center of earthquake engineering. Indian Institute of Technology Kanpur, 2007

16. Karantoni F B, Fardis M N, Vintzileou E, Harisis A. Effectiveness of Seismic Strengthening Interventions. In: Proceedings of the International Conference on Structural Preservation of the Architectural Heritage, Rome, 1993, 549–556

17. EN 1996–1-1, 2005. Eurocode 6: Design of Masonry Structures-Part 1–1: General Rules for Reinforced and Unreinforced. Masonry Structures. Europ. Comm. for Standardization: Brussels

18. EN 1998–3:2020:E. Eurocode 8, Design of Structures for Earthquake Resistance- Part 3: Assessment and retrofitting of Buildings, Brussels: European Committee for Standardization. Brussels

19. Theodoulidis N, Karakostas Ch, Lekidis V, Makra K, Margaris B, Morfidis K, Papaioannou Ch, Rovithis E, Salonikios T, Savvaidis A. The Cephalonia, Greece, January 26 (M6.1) and February 3, 2014 (M6.0) earthquakes: near-fault ground motion and effects on soil and structures. Bulletin of Earthquake Engineering, 2016, 14(1): 1–38

20. Clough R.W., Penzien J. Dynamics of Structures, New York: Mc Graw Hill, 1975

21. Karantoni F, Papadopoulos M, Pantazopoulou S J. Simple seismic assessment of traditional unreinforced masonry buildings. International Journal of Architectural Heritage, 2016, 10(8): 1055–1077

22. Karantoni F.V., Pantazopoulou S. J. Criteria guiding seismic upgrading of traditional masonry buildings. In: Proceedings 12th Canadian Masonry Symposium, Vancouver, 2013

23. Pardalopoulos S, Pantazopoulou S J, Ignatakis Ch. 2016, "Practical seismic assessment of unreinforced masonry historical buildings. Earthquakes and Structures, 2016, 11(2): 195–215

24. Marques R, Lourenço P B. Possibilities and comparison of structural component models for the seismic assessment of modern unreinforced masonry buildings. Computers & Structures, 2011, 89(21–22): 2079–2091

25. Page A W. The biaxial compressive strength of brick masonry. Proceedings- Institution of Civil Engineers, 1981, 71(Part 2): 893–906

26. Page A W. The strength of brick masonry under biaxial tension-compression. Int J of Mason Constr, 1983, 3(1): 26–31

27. Ganz H R, Thurlimann B. Test on the biaxial strength of masonry. Report No. 7502–3 Institute of Structural Engineering, Zurich, 1982

28. Mann W, Müller H. Nachrechnung der Wandversuche mit einem erweiterten Schubbruchmodell unter Berücksichtigung der Spannungen in den Stossfugen, Anlage 2 zum Forschungsbericht: Untersuchungen zum Tragverhalten von Mauerwersbauten unter Erdbebeneinwirkung, T.H. Darmstadt, 1986

29. Lourenço P B, Rots J G. A multi-surface model for the analysis of masonry structures. Journal of Engineering Mechanics, 1997, 123 (7): 660–668

30. Ottosen N. A failure criterion for concrete. Journal of Engineering Mechanics, 1977, 103(4): 527–535

31. Grünthal G. European Macroseismic Scale 1998 (EMS-98). Centre Européen de Géodynamique et de Séismologie, Luxembourg, Luxembourg, 1998

32. Karantoni F, Tsionis G, Lyrantzaki F, Fardis M N. Seismic Fragility of regular masonry buildings for in-plane and out-of-plane failure. Earthquakes and Structures, 2014, 6(6): 689–713

33. Marques R, Lourenço P B. Unreinforced and confined masonry buildings in seismic regions: Validation of macro-element models and cost analysis. Engineering Structures, 2014, 64: 52–67